

Sodium dodecyl sulfate micelles: accurate analysis of small-angle x-ray scattering data through form factor and atomistic molecular dynamics modelling

Article

Published Version

Creative Commons: Attribution 4.0 (CC-BY)

Open Access

Hamley, I. W. ORCID: <https://orcid.org/0000-0002-4549-0926>
and Castelletto, V. (2024) Sodium dodecyl sulfate micelles:
accurate analysis of small-angle x-ray scattering data through
form factor and atomistic molecular dynamics modelling.
Colloids and Surfaces A: Physicochemical and Engineering
Aspects, 696. 134394. ISSN 1873-4359 doi:
10.1016/j.colsurfa.2024.134394 Available at
<https://centaur.reading.ac.uk/116677/>

It is advisable to refer to the publisher's version if you intend to cite from the work. See [Guidance on citing](#).

To link to this article DOI: <http://dx.doi.org/10.1016/j.colsurfa.2024.134394>

Publisher: Elsevier

All outputs in CentAUR are protected by Intellectual Property Rights law, including copyright law. Copyright and IPR is retained by the creators or other copyright holders. Terms and conditions for use of this material are defined in

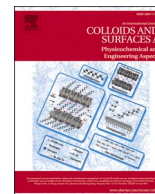
the [End User Agreement](#).

www.reading.ac.uk/centaur

CentAUR

Central Archive at the University of Reading

Reading's research outputs online

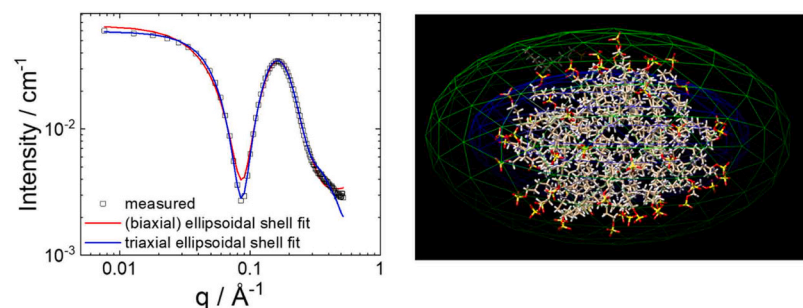


Sodium dodecyl sulfate micelles: Accurate analysis of small-angle X-ray scattering data through form factor and atomistic molecular dynamics modelling

Ian W. Hamley^{*}, Valeria Castelletto

School of Chemistry, Food Biosciences and Pharmacy, University of Reading, Whiteknights, Reading RG6 6AD, UK

GRAPHICAL ABSTRACT



ARTICLE INFO

Keywords:

Micelles
Surfactants
Self-assembly
Saxs
Molecular Dynamics
Computer Simulations

ABSTRACT

The structure of micelles of sodium dodecyl sulfate (SDS) is probed via analysis of small-angle x-ray scattering (SAXS) data with the aim to fit the data over an extended wavenumber q range. This provides detailed information on the micelle shape, which can be described as a polydisperse triaxial ellipsoidal core-shell structure according to model form factor fitting. This model was necessary to fit the data over a wide q range, which is not accurately represented by simpler models such as biaxial ellipsoidal core-shell structures. Data for SDS (at fixed concentration) in a NaCl concentration series revealed increasing structure factor effects with decreasing salt concentration. This reflects decreased charge screening on the headgroups. The structure factor could be modelled using a simple hard sphere structure factor. The analysis of form factor was complemented by atomistic molecular dynamics (MD) simulations, starting from an unbiased initial configuration of a defined number of molecules in a box. The MD configurations were used to calculate the form factor using the software CRY SOL (for small-angle scattering analysis of solution scattering, traditionally for proteins, here for micelles) and accounting for the boundary layer hydration effects. Good agreement with experimental data was found for systems with association numbers close to $p = 60$. This association number is consistent with that obtained from analysis of the form factor (in the case where structure factor effects could be neglected) and from model-free analysis of the forward scattering intensity. It is also in agreement with prior literature and our findings in regard to form factor parameters are also compared to previous reports.

^{*} Corresponding author.

E-mail address: I.W.Hamley@reading.ac.uk (I.W. Hamley).

<https://doi.org/10.1016/j.colsurfa.2024.134394>

Received 15 April 2024; Received in revised form 13 May 2024; Accepted 26 May 2024

Available online 28 May 2024

0927-7757/© 2024 The Authors. Published by Elsevier B.V. This is an open access article under the CC BY license (<http://creativecommons.org/licenses/by/4.0/>).

1. Introduction

Sodium dodecyl sulfate (SDS), also known as sodium lauryl sulfate (SLS), is a canonical anionic surfactant, widely used in commercial cleaning products such as washing-up liquid and in science and technology for applications such as cell membrane solubilization. As such, its basic physico-chemical properties have been extensively studied including micellization, which occurs above a critical micelle concentration (CMC) that is dependent on temperature and on the presence of salt or other additives. The CMC can be obtained from concentration-dependent measurements of surface tension, conductivity and other colligative properties [1–3].

The structure of SDS micelles has been investigated through small-angle scattering, both small-angle X-ray scattering (SAXS) and small-angle neutron scattering (SANS) with a wide variety of different analyses [4–13]. These methods [14] are suitable to probe micelle structure on the appropriate length scales from tens of Ångströms to atomic packing features, provided that the measurements extend over a sufficiently wide range of wavenumbers $q = 4\pi\sin\theta/\lambda$. The data at low concentration can be fitted to a suitable form factor to represent the shape of the micelles, i.e. at sufficiently low concentration, structure factor effects due to inter-micellar correlations can be neglected. A common feature revealed by much modelling is that the micelles (in water or solutions with low salt concentration) are not spherical and can be modelled as ellipsoids, either oblate or prolate. At high NaCl concentration (1 M and above), SAXS indicates the formation of wormlike micelles [10]. The transition from globular to worm-like micelles was studied by time-resolved (stroboscopic) SAXS using stopped flow mixing of SDS and concentrated salt solutions [10].

SDS micellization has also been studied via molecular dynamics (MD) computer simulations. In an early study, Shelley *et al.* reported MD on SDS micelles (with association number $p = 42$) which remained approximately spherical. The alkyl chain conformation and counterion distribution were computed, among other micellar properties [15]. Mackerell reported that SDS micelles remain spherical based on simulations using the CHARMM22 force field starting from a model of a spherical micelle with $p = 62$ [16]. Significant mobility of the headgroups was observed, although with limited conformational flexibility of the core lipid chains. Bruce *et al.* performed MD (Amber parm98 force field) on SDS micelles with $p = 60$, initially examining the micelle structure and counterion distribution, which revealed slightly anisometric micelles, the molecules not all being arranged radially [17]. A companion paper focused on water structuring (hydrogen bonding network) near the headgroups [18].

Okazaki and coworkers used MD simulations (CHARMM force field) to compute the potential energy (changes upon addition of monomers) of SDS of different association numbers along with a free energy model to find the optimal association number $p = 57$ [19]. These MD simulations also provided the free energy of water permeation into the micelle core [20], and micelle structural properties such as evidence for a prolate shape and a preferred coordination number of sulfur atoms (from headgroups) [21]. An ellipsoidal shape of SDS micelles was also noted in MD simulations (using an Amber force field) with $p = 60$, along with other structural properties of SDS micelles compared to those of SDBS (sodium dodecylbenzene sulfonate) [22]. An association number $p = 60$ was used in MD simulations (GROMOS 45a3 force field) of the interactions of poly(ethylene oxide) with SDS micelles [23]. Coarse grained MD was employed by Gao *et al.* in their study of SDS micelles [24], while coarse graining using MARTINI was performed for SDS also with $p = 60$, which revealed a significantly prolate ellipsoidal shape for the micelles, and reasonable agreement for other micelle structural properties was obtained compared to atomistic simulations [25]. Chun *et al.* performed MD on SDS micelles with $p = 60$ using a full atomistic model with Dreiding potential [26]. Structural parameters of the micelle were obtained, and it was noted that a significant fraction of the micelle surface apparently contains hydrophobic alkyl chains and that the SDS

molecules are not straight nor aligned radially from the micelle centre. The potential of mean force to extract SDS molecules from micelles was also calculated.

Storm *et al.* used the CHARMM36 force field in MD simulations along with an analytical model for intermolecular interactions between molecular surfaces based on polarization densities to calculate the distribution of association numbers of SDS (and cationic surfactant CTAB) and radial density profiles for the micelles were calculated based on different aggregation number over ranges spanning $p = 54$ –74 [27]. In a companion work, micelle/water partition coefficients were also evaluated [28]. The effect of the force field in MD simulations of SDS has been carefully examined using CHARMM36, OPLS-AA, and OPLS-UA force-fields for different association numbers [29]. Little difference in the overall micelle structure (with ellipsoidal shape) was observed using the different force fields for $p = 60$ or 100, although significant differences were observed for larger micelles (for example, differences in the final morphology).

Here, we aim to improve the modelling of SAXS data from the model surfactant system SDS. Synchrotron SAXS data for SDS in water and in (relatively dilute) aqueous NaCl solution is analysed over a wider q range than the truncated range presented in many papers, to provide a more accurate and detailed analysis of the micellar structure through detailed form factor fitting as well as complementary MD simulations. We present the first study using unbiased MD simulations to compute the SAXS form factor which proves to be in good agreement with measurements, for a suitable association number and when boundary layer effects are considered. The MD micelle shape envelope is in good agreement with that obtained from fitting the data with a polydisperse triaxial ellipsoidal core-shell form factor. Interesting structure factor effects are also noted from a salt concentration series of measurements and corresponding fits to the data. The SAXS profile is computed from unbiased MD simulations which start from a box of SDS molecules of defined association number. The association number is consistently obtained from SAXS data modelling (in salt-free or low NaCl concentration solutions) as well as the MD modelling of the form factor, and is in agreement with prior literature from small-angle scattering and other experiments and MD simulations.

In a pioneering study, Edler and coworkers presented an atomistic model for the structure of micelles of the cationic surfactant dodecyltrimethylammonium bromide (DTAB) based on wide-angle neutron scattering data [30]. The data extend to $q = 20 \text{ Å}^{-1}$ and several data sets were obtained using solvent and surfactant contrast variation to maximise the information content. The atomistic empirical potential structure refinement (EPSR) modelling employed is a variant of the reverse Monte Carlo (RMC) method. The model started from a random assembly of 64 molecules. In contrast to molecular dynamics (MD) simulations, EPSR allows the molecules to have intramolecular disorder, since each molecule independently samples a harmonic potential. The disadvantage of this method is the complexity of the work flow [31] and the specification of the force field parameters [32], whereas MD can be performed using widely used packages such as GROMACS, NAMD, Amber etc, with established force fields. A recent study on a different micellar system, *n*-dodecyl- β -D-maltoside (DDM), highlights the need to measure and model small-angle scattering (SAS) data over a sufficient q range (including relatively wide angles, up to $q = 0.6 \text{ Å}^{-1}$) to fit the form factor [33]. The authors showed that complementary atomistic MD (constrained by the experimental SAXS data) was required to fully fit the data, even if micelle asymmetry, interfacial density distribution, and fluctuations were considered in form factor models (using a triaxial ellipsoid model) [33]. MD can be used to provide additional information on the radial density distribution and effects such as surface hydration (e.g. solvent-accessible surface area, SASA) and the association number (from the micelle volume enclosed by the SASA).

Our study indicates that the form factor of SDS micelles over an extended q -range is better represented by a triaxial core-shell ellipsoid than biaxial ellipsoidal models used in the majority of prior studies

[6–13]. This is complemented by the MD simulations which were developed to be consistent with the constraint of the measured SAS data, allowing for the boundary layer hydration. The MD simulations were performed unbiased, starting from a random box of SDS molecules (of different association numbers) as well as initial spherical micelle model states. The unbiased MD simulations show the rapid development of stable micelles over a range of association numbers, the best value being obtained by comparison to the measured SAXS data. These models (and those starting from initial spherical micelle model structures) showed the development of anisotropic micelle structures, consistent with the SAXS form factor fitting.

2. Experimental

2.1. Materials and methods

2.1.1. Materials and sample preparation

Sodium dodecyl sulfate was obtained from BDH (Poole, UK) with 99% purity. Solutions of NaCl in MilliQ water or pure MilliQ water were used as a solvent to dissolve weighted amounts of SDS. The mixture was then stirred to produce a homogeneous solution.

2.1.2. Small-angle X-ray scattering experiments (SAXS)

Synchrotron SAXS experiments on solutions were performed using a BioSAXS setup on BM29 at the ESRF (Grenoble, France) [34]. A few microlitres of samples were injected via an automated sample exchanger at a slow and very reproducible rate into a quartz capillary (1.8 mm internal diameter), in the X-ray beam. The quartz capillary was enclosed in a vacuum chamber, to avoid parasitic scattering. After the sample was injected in the capillary and reached the X-ray beam, the flow was stopped during the SAXS data acquisition. The q range was $0.005\text{--}0.48\text{ \AA}^{-1}$, with $\lambda = 1.03\text{ \AA}$ and a sample-detector distance of 2867 mm. The images were obtained using a Pilatus3–2 M detector. Data processing (background subtraction, radial averaging) was performed using dedicated beamline software ISPyB.

Form factor fitting was performed with SASfit [35,36] using a polydisperse core-shell triaxial ellipsoid model, and a hard sphere structure factor, as required.

2.2. Molecular dynamics simulations

Molecular dynamics simulations were performed using Gromacs [37] (version 2020.1-Ubuntu-2020.1–1). SDS molecules (number $p = 55, 58, 60, 62, 65, 100$ and 140) were randomly packed in a $(40\text{ nm})^3$ box using Packmol [38], and in the case of $p = 60$, spherical micelles were generated in Packmol as an additional comparative initial state. The SDS molecular structure (pdb file) was obtained from the CHARMM-GUI server [39] and simulations were performed using the CHARMM27 force field [40,41] using the included force field parameters for SDS. The system was solvated using spc216 water. Each system was neutralized using a matching number of Na^+ counterions. After energy minimization and 100 ps relaxation stages in the NVT and NPT ensembles, the final simulations were carried out in the NPT ensemble using a leap-frog integrator with 1,000,000 steps of 2 fs up to 1000 ps. The temperature was maintained at 300 K using the velocity-rescale (modified Berendsen) thermostat [42] with a coupling constant of 10 steps. The pressure was maintained at 1 bar using the Parinello-Rahman barostat [43] and periodic boundary conditions were applied in all three dimensions. The Particle Mesh Ewald scheme [44,45] was used for long-range electrostatics. Bonds were constrained using the LINCS algorithm [46] and the Verlet cutoff scheme [47] was used. Coulomb and van der Waals cutoffs were 1.0 nm.

3. Results

SAXS data was measured for SDS under several conditions of

surfactant and salt concentration. Taking a data set for SDS at high salt concentration (2 wt% SDS in 0.4 M NaCl) provided a test data set with minimal structure factor effects apparent, i.e. providing a dataset to fit the form factor. Various models for the form factor fitting were attempted. A biaxial ellipsoidal core-shell form factor was found to either not accurately describe the depth of the form factor minimum (Fig. 1) or to not properly describe the scattering at high q and/or to have unphysical fit parameters (SI Fig. S1, fit parameters listed in SI Table S1). However, a triaxial core-shell structure (with polydispersity in the core short axis as well as shell thickness) was found to provide a good fit to the data across the whole measured wavenumber range $q = 0.007\text{--}0.52\text{ \AA}^{-1}$ (Fig. 1) with only a slight underestimation of the scattering at high q which may be due to a scattering contribution from unaggregated molecules or the effect of local structure. The χ^2 and other statistical parameters from the fitting are listed in SI Table S2 (and were significantly lower for the core-shell triaxial ellipsoid than the biaxial ellipsoid models), while residuals are plotted in SI Fig. S2. The triaxial ellipsoidal core-shell form factor was then used in subsequent fitting of data measured for a series of NaCl concentrations with the SDS concentration fixed at 2 wt%. This data along with the form factor fits is shown in Fig. 2. The form factor fit parameters are listed in Table 1. The micelles are characterized by one axis (c) being notably shorter than the other two and can thus be classified as “pseudo-oblate”.

There are significant structure factor effects in all data except the highest salt concentration (0.4 M NaCl) studied where only small structure factor effects were noted. This was satisfactorily accounted for the fitting using a hard sphere structure factor [11,14,48,49]. This has fewer parameters than other models such as the Hayter-Penfold model used to describe charged colloids. The structure factor influences the form factor parameters, in particular the ellipsoid dimensions a and b (especially for the data in the absence of salt which has large structure factor effects). The hard sphere radius and volume fraction grow monotonically as salt concentration decreases (Table 1).

The ellipsoid dimensions from the form factor analysis were used to calculate the micelle volume, from which the apparent association number p_{app} was obtained. The volume of the hydrophobic moiety can be estimated using the equation due to Tanford for the volume per lipid chain [50], $v_l = 27.4 + 26.9 n$ (where n is the number of carbons in the lipid chain excluding the terminal CH_3 group, i.e. $n = 11$ and v_l is in units of \AA^3), which yields $v_l = 323.3\text{ \AA}^3$. The volume of a triaxial ellipsoid with semi-axes a, b, c (the micelle core volume from the SAXS form factor fitting) is given by $v_{\text{core}} = \frac{4}{3}\pi abc$, and the corresponding values are

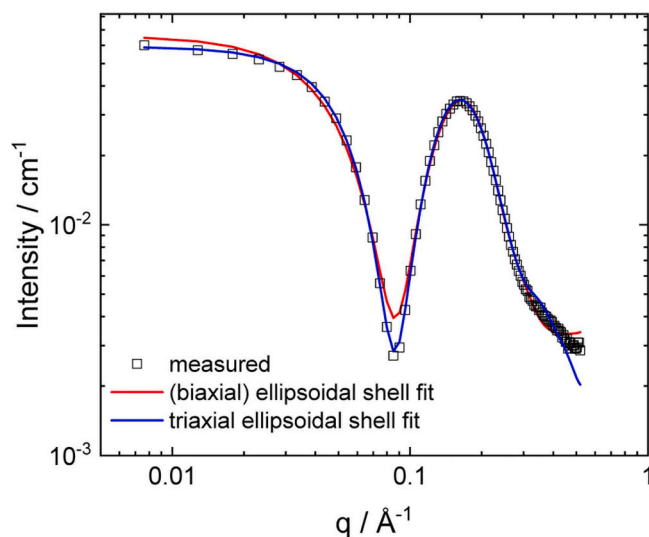


Fig. 1. SAXS data measured for 2 wt% SDS in 0.4 M NaCl (open symbols) along with fitted form factors (red and blue lines, described in text). For ease of visualization a reduced data set is shown (binning of groups of 10 data points).

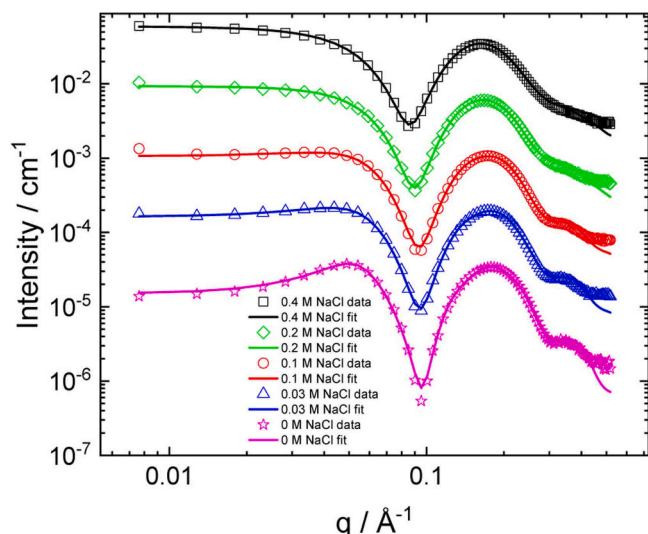


Fig. 2. SAXS data measured for 2 wt% SDS in the absence or presence of NaCl at the concentrations indicated (open symbols) along with fitted form factors (solid lines). For ease of visualization a reduced data set is shown (binning of groups of 10 data points) and with respect to the top dataset (0.4 M NaCl) the lower ones are offset by division by successive factors of 5 (i.e. 5, 25, 125 and 625).

Table 1

Results from form factor fitting using a triaxial core-shell ellipsoid form factor and calculated micelle volume and apparent association number p_{app} .

Conditions	2 wt%	2 wt% SDS	2 wt% SDS	2 wt% SDS	2 wt% SDS
Parameters	SDS in H ₂ O (20 °C)	in 0.03 M NaCl (20 °C)	in 0.1 M NaCl (20 °C)	in 0.2 M NaCl (20 °C)	in 0.4 M NaCl (20 °C)
$c / \text{\AA}$	13.2	13.1	12.9	13.1	12.8
$b / \text{\AA}$	15.8	16.6	16.3	18.9	19.4
$a / \text{\AA}$	23.3	24.2	23.7	25.9	27.6
$t_{shell} / \text{\AA}$	8.0	8.0	8.8	8.1	8.1
$\sigma / \text{\AA}$	0.0939	0.0939	0.1000	0.0095	0.0254
$\eta_{core} / \text{cm}^{-1}$	-1.3×10^{-5}	-1.3×10^{-5}	-1.3×10^{-5}	-1.2×10^{-5}	-1.3×10^{-5}
$\eta_{shell} / \text{cm}^{-1}$	1.0×10^{-5}	1.0×10^{-5}	9.6×10^{-6}	1.1×10^{-5}	1.1×10^{-5}
BG / cm^{-1}	9.6×10^{-5}	6.3×10^{-4}	1.0×10^{-3}	1.1×10^{-3}	1.6×10^{-3}
$R_{HS} / \text{\AA}$	52.5	48.1	46.3	43.3	44.5
ϕ	0.213	0.137	0.114	0.053	0.033
$v_{core} / \text{\AA}^3$	20,355	22,044	20,874	26,861	28,708
p_{app}	63.0	68.1	64.6	83.0	88.8

Key: Form factor: a, b, c : ellipsoid semi-axis lengths, t_{shell} : shell thickness, σ : log-normal distribution width for polydispersity in c and t_{shell} , η_{core} : core scattering contrast (electron density), η_{shell} : shell scattering contrast (electron density), BG: constant background. **Structure factor:** R_{HS} , hard sphere radius, ϕ effective volume fraction.

listed in Table 1. This can be used to calculate the apparent association number as $p_{app} = v_{core}/v_l$. The values listed in Table 1 show that SAXS data provides values of p_{app} in reasonable agreement with the association number $p = 60$ obtained from other analyses of the data (discussed below) and MD simulations. The value obtained from the form factor parameters is higher at high salt concentration (0.2 M and 0.4 M NaCl, Table 1), which may be a real effect resulting from enhanced association possible due to screening of the headgroup charge at high salt concentration.

The form factor fitting was able to fit the data over an extended q range, with some deviation at high q , but does not provide an atomistic picture of the micelle structure. MD simulations were then performed which provide atomistic detail of the micelle configuration, and the form factor was computed for comparison with the analytical model fits. MD simulations were performed using the CHARMM27 force field, starting

from initial random configurations with defined association numbers $p = 55, 58, 60, 62, 65, 100$ and 140 . In all cases, very rapid assembly into anisotropic micelles was observed, even during the initial “equilibration” constant NVT part of the simulation. Frames from this run for $p = 60$ are shown in SI Fig. S3. A structure after a full 1000 ps MD run is shown in Fig. 3 and a movie showing the trajectory during this run is provided as SI Movie S1. Convergence of the simulations is confirmed from the convergence of the calculated SDS atom root-mean-square deviation (RMSD) and solvent-associated surface area (SASA) and SASA-enclosed volume (SI Fig. S4). Since the SAXS data indicates that the association number is around $p = 60$, the two higher p values ($p = 100$ and $p = 140$) are not considered further, although anisotropic micelle-like structures were observed to be stable for these systems.

Using the atomic coordinates from the MD simulations (in pdb file format), the SAXS profile was computed using CRYSOLO which is part of the ATSAS software (mainly designed for protein SAS data modelling) that performs calculations using the Debye equation, allowing for the scattering effects due to displaced solvent and surface hydration [51–53]. Good agreement with experimental data was observed (exemplified in Fig. 4, which shows data measured for a very dilute and salt-free SDS solution where structure factor effects are minimal) noting that there is some variation in the computed profiles from one MD run to another and allowing for variation in association number (likely to be the case in practice) as shown in SI Fig. S5. These calculations particularly highlighted the need to account for the boundary layer, as evident from SI Fig. S5 comparing profiles calculated with and without head group sulfate oxygen atoms. An overlay of the micelle structure from MD for $p = 60$ along with the form factor core-shell ellipsoid structure (using the parameters from the fit for the 0.4 M NaCl solution from Table 1) is shown in Fig. 5a. Different projections of the ellipsoidal core-shell structure are also illustrated (Fig. 5b). From Fig. 5a, it is clear that there is good overlap between the core ellipsoid and the $p = 60$ SDS micelle structure from MD simulations. The outer shell in the form factor model must be present to account for fluctuations in the micelle configuration, shape and association number as well as the presence of the Na^+ counterion shell and bound water.

As a check on self-consistency, the association number was obtained from the micelle volume enclosed by the SASA (SI Fig. S6). This was computed from MD data for SDS micelles with $p = 60$ giving a volume $v_{SASA} = 20.23 \times 10^3 \text{\AA}^3$ (from UCSF Chimera), divided by the tail volume obtained from the Tanford equation (discussed above) $v_l = 323.3 \text{\AA}^3$ leads to $p = v_{SASA}/v_l = 62$. This also provides an indirect check of the accuracy of the Tanford approximation (the volume of the sulfate headgroup appears not to significantly influence this).

As a further independent check, the association number can be obtained in a model-independent way from the forward scattering intensity [14,54]. The measured SAXS data presented here is in absolute units (cm^{-1}) and the forward scattering (at $q = 0$) can be written as [12]:

$$I(0) = c_{mic} M_{mic} [r_0 v_p (\rho_{SDS} - \rho_0)]^2 / N_A \quad (1)$$

Here c_{mic} is the concentration of micelles, M_{mic} is the micelle molar mass, r_0 is the classical electron radius ($0.28179 \times 10^{-12} \text{ cm e}^{-1}$), v_p is the SDS partial specific volume, ρ_{SDS} and ρ_0 represent the SDS and solvent (water) electron density and N_A is Avogadro’s number. Here we wish to obtain the micelle molar mass and hence p . Rearranging Eq. (1) gives:

$$M_{mic} = \frac{I(0) N_A}{c_{mic} [r_0 v_p (\rho_{SDS} - \rho_0)]^2} \quad (2)$$

SDS contains 145 electrons in a molecular volume $v_{mol} = 390.3 \text{\AA}^3$ [12], i.e. the electron density is $\rho_{SDS} = 0.372 \text{ e \AA}^{-3}$. The electron density of water is taken as $\rho_0 = 0.333 \text{ e \AA}^{-3}$. Taking a concentration $c_{mic} = 2 \text{ wt \%}$ (0.02 g cm^{-3}) and with $v_p = 0.815 \text{ cm}^3 \text{ g}^{-1}$ [12], and using $I(0) = 0.07 \text{ cm}^{-1}$ (Guinier extrapolation of the data in Fig. 1) leads to $M_{mic} =$

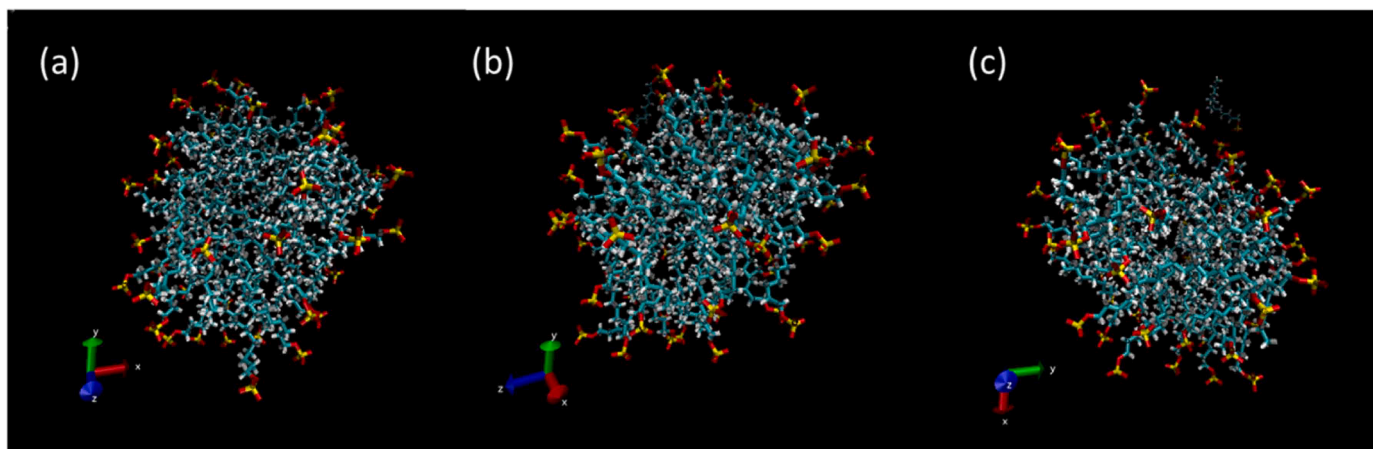


Fig. 3. Different projections of a simulated SDS micelle with $p = 60$. Note the presence of an unassociated molecule (visible in the back in part c).

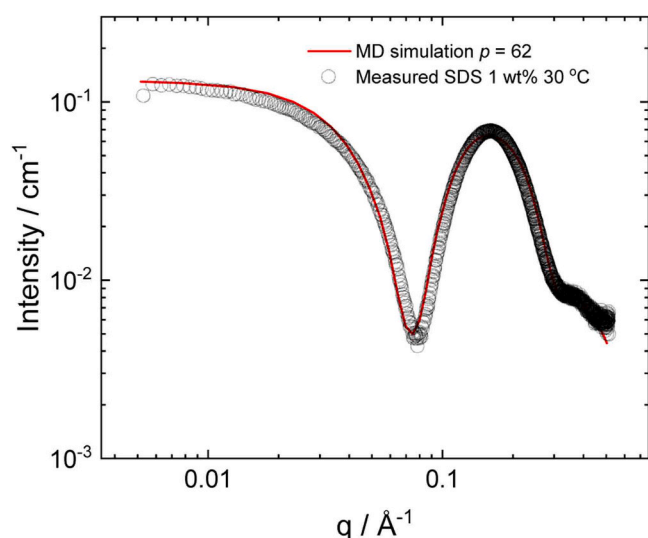


Fig. 4. Comparison of measured data for 0.01 wt% SDS (30 °C) with CRYSOLE-calculated SAXS profile from an MD simulation with $p = 62$. A flat background scattering $BG = 10^{-3}$ was included to improve the high q fit of the calculated profile from MD coordinates.

$2.63 \times 10^4 \text{ g mol}^{-1}$, i.e. $p = 91$. This is clearly an overestimate based on comparison to the form factor fitting, and compared to MD and may reflect the presence of residual structure factor effects in the data.

4. Discussion

The micelle structure parameters obtained here are compared with previous data obtained from SANS and SAXS studies on SDS. Micelle structural parameters from form factor fitting from selected studies with detailed form factor analysis are listed in Table 2.

Detailed SANS measurements were performed for SDS in NaBr solutions and different form factor models were applied depending on SDS and NaBr concentrations [5]. At low NaBr concentration, the data could be fitted with an ellipsoidal form factor, at 0.2–0.4 M NaBr, a triaxial ellipsoidal model was used and at higher [NaBr], a wormlike chain model was used. Fit parameters for the 0.2 M NaBr solution are included in Table 2. The SANS data does not show form factor maxima/minima due to the contrast in D_2O , and the lower resolution of the SANS measurements. Another SANS study of SDS in aqueous solutions with and without the salt *p*-toluidine hydrochloride included form factor fitting using a prolate ellipsoid model [7]. The data shows strong structure factor effects in the 50 mM (1.4 wt%) SDS samples studied in D_2O in the absence of salt (as in the prior SANS study [5]) or at low salt concentration, this being accounted for by inclusion of a rescaled mean spherical approximation structure factor. Micelle growth upon increase of the salt concentration was accounted for by extension along the long axis of the ellipsoid in the form factor fits [7].

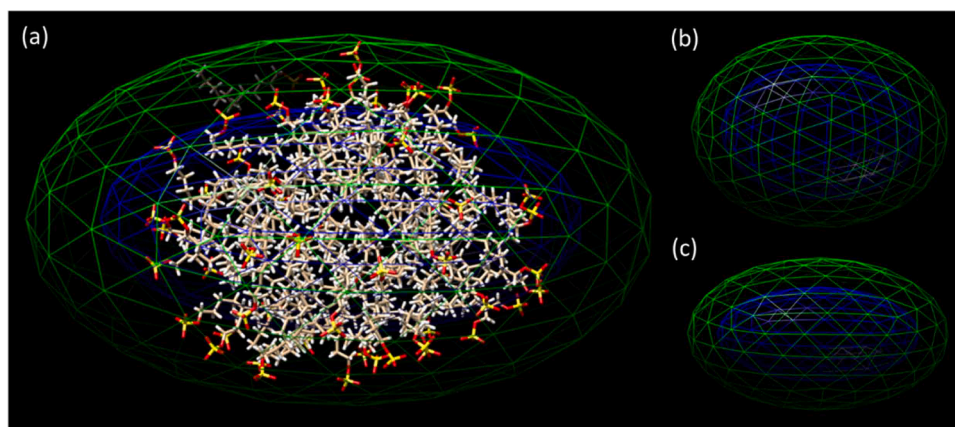


Fig. 5. (a) Overlay of MD configuration of SDS micelle for $p = 60$ with form factor ellipsoids (core: blue, outside including shell: green) using the parameters for 2 wt % SDS 0.4 M NaCl (Table 1), (b,c) Two projections of the core-shell ellipsoids.

Table 2

Comparison of current form factor fit with selected previous analyses. Unless specified, “ellipsoid” refers to a biaxial ellipsoid.

Conditions and model	1 wt% SDS in 0.2 M NaBr (D ₂ O) (40 °C)	2.3 wt% SDS in D ₂ O (40 °C)	1.4 wt% SDS in D ₂ O (25 °C)	1 wt% SDS in D ₂ O (25 °C)	2.3 wt% SDS in D ₂ O (40 °C)
	<i>Monodisperse triaxial ellipsoid</i> [5]	<i>Monodisperse ellipsoid</i> [6]	<i>Monodisperse ellipsoid</i> [7]	<i>Core-shell ellipsoid</i> [8]	<i>Monodisperse ellipsoid</i> [13]
Parameters	“Oblate-like” ellipsoid	Prolate ellipsoid	Prolate ellipsoid	Prolate ellipsoid	Oblate ellipsoid
$a / \text{\AA}$	13.8	24.0	25.0 ± 2.1	16.7	13.6
$b / \text{\AA}$	23.0	15.7	16.7^a	20.9	20.6
$c / \text{\AA}$	25.3	-	-	-	-
ε	N/A	1.53	1.50	1.25	0.661
$t_{\text{shell}} / \text{\AA}$	-	-	-	3.2	-

Conditions and model	1% SDS in D ₂ O (21 °C)	0.5% SDS in 0.5 M NaCl	0.63% SDS in 50 mM HEPES buffer, pH 7.8, 0.15 M NaCl (20 °C)	1 wt% SDS (20 °C)
	<i>Monodisperse ellipsoid</i> [9]	<i>Ellipsoidal core-shell</i> [10]	<i>Core-shell ellipsoid with polydispersity</i> [12]	<i>Core-shell ellipsoid (with smearing)</i> [11]
Parameters	Oblate ellipsoid	Prolate ellipsoid	Prolate ellipsoid	Oblate ellipsoid
$a / \text{\AA}$	15.0	31.2	31.2 ± 2.0	16.5
$b / \text{\AA}$	21.8	16.0 ± 0.2	17.8 ± 0.02	22.8
$c / \text{\AA}$	-	-	-	-
ε	0.688	1.95 ± 0.07	1.75 ± 0.11	0.76
$t_{\text{shell}} / \text{\AA}$	-	7.3 ± 0.2	4.85 ± 0.17	5.5

Key: a, b, c : ellipsoid semi-axis lengths (in the case of a biaxial ellipsoid $b = c$), ε : aspect ratio (ellipticity, for biaxial only), t_{shell} : shell thickness^a Constrained based on hydrophobic chain length

The ambiguity in fitting SAXS data for SDS (and cesium dodecyl sulfate) to either prolate or oblate ellipsoid form factor models was addressed by Vass *et al.* [13] who in fact showed that in a certain q range, oblate and prolate ellipsoid form factors cannot be distinguished. They argue that the prolate conformation is likely to be favoured, based on the physical meaning of form factor fit parameters as well as the observed phenomenon of micelle elongation at high salt content. However, parameters from a fit to an oblate ellipsoid form factor are included in Table 2 (the measured SANS data also required allowance for structure factor) [6,13] since our analysis is consistent with this shape. Hammouda analysed SANS data for SDS in D₂O using a model of oblate ellipsoids for the form factor and a mean spherical approximation (in the Ornstein-Zernike equation) for the structure factor [9]. Temperature-dependent measurements were performed which reveal a nearly linear decrease in ellipsoid semi-axis lengths with temperature (in the range 11 – 87 °C). Jensen *et al.* fitted SAXS data (up to $q = 0.2 \text{ \AA}^{-1}$) for SDS in NaCl solutions (with strong form factor maxima/minima) using a model of prolate core-shell ellipsoidal micelles (it is not clear whether or how polydispersity was included in the model but uncertainty values are provided, as listed in Table 2) [10]. Recent SAXS data for SDS micelles has been fitted with an (oblate) ellipsoidal core-shell model as part of a study on the interaction of common surfactants with lipid membranes [11]. Structure factor effects had to be accounted for, and this was done using a hard sphere model.

In summary, Table 2 shows a reasonable consistency between the parameters for the more recent SAS form factor fitting using various models for prolate ellipsoids. Our fitting using a triaxial core-shell ellipsoid form factor provides accurate fits over an extended q range, in contrast to some previous SAS data analysis which uses a less extended q range. The ellipsoid parameters from our fits are in the same general range as those previously reported, although they do differ in detail (comparing data in Table 1 and Table 2).

Based on their analysis of SAXS data for micelles of a series of nonionic glucosides, mannosides and zwitterionic phosphocholines, Lipfert *et al.* propose that the position of the secondary maximum in the form factor of micelles (prolate or oblate ellipsoids in their case) can be associated with the shortest center-center separation of surfactant head groups [54]. For the data here (2 wt% SDS, no salt) the maximum is at $q = 0.161 \pm 0.002 \text{ \AA}^{-1}$ (Fig. 1) corresponding to $d = 39.0 \pm 0.5 \text{ \AA}$. This is reasonably close to $2\left(c + \frac{t_{\text{shell}}}{2}\right) = 34.0 \pm 3.4 \text{ \AA}$ from our model (Table 1),

so this estimation appears to be an acceptable first approximation for SDS.

The calculated association numbers in Table 1 are in good agreement with the literature for 0.5 – 1 wt% SDS in aqueous or dilute salt solution at around 20 °C for which values in the range $p = 59 - 70$ are generally reported [5,6,8,9], although higher values have been reported, for example $p = 79$ by Hassan *et al.* (salt-free D₂O solution) [7], $p = 84$ (0.03 M solution 25 °C) from SANS measurements in D₂O [4], or $p = 90$ from SAXS data in HEPES buffer [12]. The value $p = 60$ is also consistent with values used in MD simulations as discussed above.

5. Conclusions

In summary we have shown that SDS micelle form factor can be accurately fitted over an extended q range using a triaxial ellipsoidal core-shell model. This fits the data significantly better than a (biaxial) ellipsoidal core-shell model with a notably improved overall fit quality. The association number deduced from this data is in good agreement with prior literature and MD simulations. Data at low salt concentrations requires allowance for structure factor. The apparent association number obtained from the form factor structure parameters in this case is significantly higher. MD simulations with $p = 60$ (and allowing for polydispersity around this value) show rapid development of micelle structure starting from a random box of SDS molecules and the equilibrated micelle structures provide computed form factors in good agreement with the measured data (at high salt concentration where structure factor can be neglected) when the boundary layer structure and hydration is accounted for. In future, MD analysis of small-angle scattering data should be combined with machine learning methods or AI to avoid *a priori* inputs such as the association number, as in the current work.

CRedit authorship contribution statement

Valeria Castelletto: Methodology, Investigation, Data curation. **Ian W. Hamley:** Writing – review & editing, Writing – original draft, Validation, Supervision, Software, Project administration, Methodology, Funding acquisition, Formal analysis, Data curation, Conceptualization.

Declaration of Competing Interest

The authors declare that they have no known competing financial interests or personal relationships that could have appeared to influence the work reported in this paper.

Data Availability

Data will be made available on request.

Acknowledgements

This work was supported by EPSRC Fellowship grant (reference EP/V053396/1) to IWH. We thank the ESRF for beamtime on BM29 (ref. MX-2513) and Mark Tully and Dihia Moussaoui for help. We acknowledge use of facilities in the Chemical Analysis Facility (CAF) at the University of Reading.

Appendix A. Supporting information

Supplementary data associated with this article can be found in the online version at [doi:10.1016/j.colsurfa.2024.134394](https://doi.org/10.1016/j.colsurfa.2024.134394).

References

- [1] D.F. Evans, H. Wennerström, *The Colloidal Domain. Where Physics, Chemistry, Biology and Technology Meet*, Wiley, New York, 1999.
- [2] R.J. Hunter, *Foundations of Colloid Science*, 2nd ed., Oxford University Press, Oxford, 2001.
- [3] I.W. Hamley, *Introduction to Soft Matter*, Revised Edition, Wiley, Chichester, 2007.
- [4] V.Y. Bezzobotov, S. Borbely, L. Cser, B. Faragó, I.A. Gladkih, Y.M. Ostanevich, S. Vass, Temperature and concentration dependence of properties of sodium dodecyl sulfate micelles determined from small-angle neutron scattering experiments, *J. Phys. Chem. B* 102 (1998) 5738–5743.
- [5] M. Bergström, J.S. Pedersen, A small-angle neutron scattering (SANS) study of tablet-shaped and ribbonlike micelles formed from mixtures of an anionic and a cationic surfactant, *J. Phys. Chem. B* 103 (1999) 8502–8513.
- [6] S. Vass, T. Gilányi, S. Borbely, SANS study of the structure of sodium alkyl sulfate micellar solutions in terms of the one-component macrofluid model, *J. Phys. Chem. B* 104 (2000) 2073–2081.
- [7] P.A. Hassan, G. Fritz, E.W. Kaler, Small angle neutron scattering study of sodium dodecyl sulfate micellar growth driven by addition of a hydrotropic salt, *J. Colloid Interface Sci.* 257 (2003) 154–162.
- [8] P.C. Griffiths, N. Hirst, A. Paul, S.M. King, R.K. Heenan, R. Farley, Effect of ethanol on the interaction between poly(vinylpyrrolidone) and sodium dodecyl sulfate, *Langmuir* 20 (2004) 6904–6913.
- [9] B. Hammouda, Temperature effect on the nanostructure of SDS micelles in water, *J. Res. Natl. Inst. Stand. Technol.* 118 (2013) 151–167.
- [10] G.V. Jensen, R. Lund, J. Gummel, T. Narayanan, J.S. Pedersen, Monitoring the transition from spherical to polymer-like surfactant micelles using small-angle x-ray scattering, *Angew. Chem., Int. Ed. Engl.* 53 (2014) 11524–11528.
- [11] V.A. Bjørnstad, R. Lund, Pathways of membrane solubilization: a structural study of model lipid vesicles exposed to classical detergents, *Langmuir* 39 (2023) 3914–3933.
- [12] A. Pozza, F. Bonneté, Analysis and modeling of SDS and DPC micelle SAXS data for membrane protein solution structure characterization, *Data Brief.* 47 (2023).
- [13] S. Vass, J.S. Pedersen, J. Plestil, P. Laggner, E. Rétfalvi, I. Varga, T. Gilányi, Ambiguity in determining the shape of alkyl sulfate micelles from small-angle scattering data, *Langmuir* 24 (2008) 408–417.
- [14] I.W. Hamley, *Small-Angle Scattering: Theory, Instrumentation, Data and Applications*, Wiley, Chichester, 2021.
- [15] J. Shelley, K. Watanabe, M.L. Klein, Simulation of a sodium dodecyl-sulfate micelle in aqueous-solution, *Int. J. Quantum Chem.* (1990) 103–117.
- [16] A.D. Mackerell, Molecular dynamics simulation analysis of a sodium dodecyl-sulfate micelle in aqueous-solution - decreased fluidity of the micelle hydrocarbon interior, *J. Phys. Chem.* 99 (1995) 1846–1855.
- [17] C.D. Bruce, M.L. Berkowitz, L. Perera, M.D.E. Forbes, Molecular dynamics simulation of sodium dodecyl sulfate micelle in water: micellar structural characteristics and counterion distribution, *J. Phys. Chem. B* 106 (2002) 3788–3793.
- [18] C.D. Bruce, S. Senapati, M.L. Berkowitz, L. Perera, M.D.E. Forbes, Molecular dynamics simulations of sodium dodecyl sulfate micelle in water: the behavior of water, *J. Phys. Chem. B* 106 (2002) 10902–10907.
- [19] N. Yoshii, K. Iwahashi, S. Okazaki, A molecular dynamics study of free energy of micelle formation for sodium dodecyl sulfate in water and its size distribution, *J. Chem. Phys.* 124 (2006).
- [20] N. Yoshii, S. Okazaki, Free energy of water permeation into hydrophobic core of sodium dodecyl sulfate micelle by molecular dynamics calculation, *J. Chem. Phys.* 126 (2007).
- [21] N. Yoshii, S. Okazaki, A molecular dynamics study of structure and dynamics of surfactant molecules in SDS spherical micelle, *Condens. Matter Phys.* 10 (2007) 573–578.
- [22] F. Palazzesi, M. Calvaresi, F. Zerbetto, A molecular dynamics investigation of structure and dynamics of SDS and SDBS micelles, *Soft Matter* 7 (2011) 9148–9156.
- [23] B.Z. Shang, Z.W. Wang, R.G. Larson, Molecular dynamics simulation of interactions between a sodium dodecyl sulfate micelle and a poly(ethylene oxide) polymer, *J. Phys. Chem. B* 112 (2008) 2888–2900.
- [24] J. Gao, W. Ge, G.H. Hu, J.H. Li, From homogeneous dispersion to micelles - a molecular dynamics simulation on the compromise of the hydrophilic and hydrophobic effects of sodium dodecyl sulfate in aqueous solution, *Langmuir* 21 (2005) 5223–5229.
- [25] S. Jalili, M. Akhavan, A coarse-grained molecular dynamics simulation of a sodium dodecyl sulfate micelle in aqueous solution, *Colloids Surf. a-Physicochem. Eng. Asp.* 352 (2009) 99–102.
- [26] B.J. Chun, J.I. Choi, S.S. Jang, Molecular dynamics simulation study of sodium dodecyl sulfate micelle: water penetration and sodium dodecyl sulfate dissociation, *Colloids Surf. a-Physicochem. Eng. Asp.* 474 (2015) 36–43.
- [27] S. Storm, S. Jakobtorweihen, I. Smirnova, A.Z. Panagiotopoulos, Molecular dynamics simulation of SDS and CTAB micellization and prediction of partition equilibria with COSMOmic, *Langmuir* 29 (2013) 11582–11592.
- [28] T. Ingram, S. Storm, L. Kloss, T. Mehling, S. Jakobtorweihen, I. Smirnova, Prediction of micelle/water and liposome/water partition coefficients based on molecular dynamics simulations, COSMO-RS, COSMOmic, *Langmuir* 29 (2013) 3527–3537.
- [29] X.M. Tang, P.H. Koenig, R.G. Larson, Molecular dynamics simulations of sodium dodecyl sulfate micelles in water-the effect of the force field, *J. Phys. Chem. B* 118 (2014) 3864–3880.
- [30] R. Hargreaves, D.T. Bowron, K. Edler, Atomistic structure of a micelle in solution determined by wide Q-range neutron diffraction, *J. Am. Chem. Soc.* 133 (2011) 16524–16536.
- [31] H. Laurent, M.D.G. Hughes, M. Walko, D.J. Brockwell, N. Mahmoudi, T.G. A. Youngs, T.F. Headen, L. Dougan, Visualization of self-assembly and hydration of a β -hairpin through integrated small and wide-angle neutron scattering, *Biomacromolecules* 24 (2023) 4869–4879.
- [32] Soper, A.K. 2017, *Empirical Potential Structure Refinement: A User's Guide*, 2017. <https://www.isis.stfc.ac.uk/OtherFiles/Disordered%20Materials/EPsR25%20Manual%202017-10.pdf>.
- [33] M.T. Ivanovic, M.R. Hermann, M. Wojcik, J. Pérez, J.S. Hub, Small-angle x-ray scattering curves of detergent micelles: effects of asymmetry, shape fluctuations, disorder, and atomic details, *J. Phys. Chem. Lett.* 11 (2020) 945–951.
- [34] P. Pernot, A. Round, R. Barrett, A.D. Antolinos, A. Gobbo, E. Gordon, J. Huet, J. Kieffer, M. Lentini, M. Mattenet, C. Morawe, C. Mueller-Dieckmann, S. Ohlsson, W. Schmid, J. Surr, P. Theveneau, L. Zerrad, S. McSweeney, Upgraded ESRF BM29 beamline for SAXS on macromolecules in solution, *J. Synchrotron Radiat.* 20 (2013) 660–664.
- [35] I. Bressler, J. Kohlbrecher, A.F. Thünemann, SASfit: a tool for small-angle scattering data analysis using a library of analytical expressions, *J. Appl. Crystallogr.* 48 (2015) 1587–1598.
- [36] J. Kohlbrecher, I. Bressler, Updates in SASfit for fitting analytical expressions and numerical models to small-angle scattering patterns, *J. Appl. Crystallogr.* 55 (2022) 1677–1688.
- [37] M.J. Abraham, T. Murtola, R. Schulz, S. Páll, J.C. Smith, B. Hess, E. Lindahl, GROMACS: high performance molecular simulations through multi-level parallelism from laptops to supercomputers, *SoftwareX* 1–2 (2015) 19–25.
- [38] L. Martínez, R. Andrade, E.G. Birgin, J.M. Martínez, PACKMOL: a package for building initial configurations for molecular dynamics simulations, *J. Comput. Chem.* 30 (2009) 2157–2164.
- [39] S. Jo, T. Kim, V.G. Iyer, W. Im, Software news and updates - CHARMM-GUI: A web-based graphical user interface for CHARMM, *J. Comput. Chem.* 29 (2008) 1859–1865.
- [40] A.D. MacKerell, D. Bashford, M. Bellott, R.L. Dunbrack, J.D. Evanseck, M.J. Field, S. Fischer, J. Gao, H. Guo, S. Ha, D. Joseph-McCarthy, L. Kuchnir, K. Kucera, F.T. K. Lau, C. Mattos, S. Michnick, T. Ngo, D.T. Nguyen, B. Prodhom, W.E. Reiher, B. Roux, M. Schlenkerich, J.C. Smith, R. Stote, J. Straub, M. Watanabe, J. Wiórkiewicz-Kucera, D. Yin, M. Karplus, All-atom empirical potential for molecular modeling and dynamics studies of proteins, *J. Phys. Chem. B* 102 (1998) 3586–3616.
- [41] N. Foloppe, A.D. MacKerell, All-atom empirical force field for nucleic acids: I. Parameter optimization based on small molecule and condensed phase macromolecular target data, *J. Comput. Chem.* 21 (2000) 86–104.
- [42] G. Bussi, D. Donadio, M. Parrinello, Canonical sampling through velocity rescaling, *J. Chem. Phys.* 126 (2007).
- [43] M. Parrinello, A. Rahman, Polymorphic transitions in single-crystals - a new molecular-dynamics method, *J. Appl. Phys.* 52 (1981) 7182–7190.
- [44] T. Darden, D. York, L. Pedersen, Particle mesh ewald - an $N \log(N)$ method for ewald sums in large systems, *J. Chem. Phys.* 98 (1993) 10089–10092.
- [45] U. Essmann, L. Perera, M.L. Berkowitz, T. Darden, H. Lee, L.G. Pedersen, A smooth particle mesh ewald method, *J. Chem. Phys.* 103 (1995) 8577–8593.
- [46] B. Hess, H.J.C. Berendsen, J. Fraaije, LINCS: A linear constraint solver for molecular simulations, *J. Comput. Chem.* 18 (1997) 1463–1472.

- [47] L. Verlet, Computer 'experiments' on classical fluids. I. Thermodynamical properties of Lennard-Jones molecules, *Phys. Rev.* 159 (1967) 98–103.
- [48] D.J. Kinning, E.L. Thomas, Hard-sphere interactions between spherical domains in diblock copolymers, *Macromolecules* 17 (1984) 1712–1718.
- [49] J.S. Pedersen, Analysis of small-angle scattering data from colloids and polymer solutions: modeling and least-squares fitting, *Adv. Colloid Interface Sci.* 70 (1997) 171–210.
- [50] C. Tanford, *The Hydrophobic Effect. Formation of Micelles and Biological Membranes*, Wiley, New York, 1980.
- [51] D. Svergun, C. Barberato, M.H.J. Koch, CRY SOL - A program to evaluate x-ray solution scattering of biological macromolecules from atomic coordinates, *J. Appl. Crystallogr.* 28 (1995) 768–773.
- [52] D.I. Svergun, M.H.J. Koch, Small-angle scattering studies of biological macromolecules in solution, *Rep. Prog. Phys.* 66 (2003) 1735–1782.
- [53] D.I. Svergun, M.H.J. Koch, P.A. Timmins, R.P. May, *Small Angle X-ray and Neutron Scattering from Solutions of Biological Macromolecules*, Oxford University Press, Oxford, 2013.
- [54] J. Lipfert, L. Columbus, V.B. Chu, S.A. Lesley, S. Doniach, Size and shape of detergent micelles determined by small-angle x-ray scattering, *J. Phys. Chem. B* 111 (2007) 12427–12438.